

## Unidirectional Growth of Lithium Sulphanilate hydrate (LS) Single crystals for Third order nonlinear applications

M. Anantharaja, N. Elavarasu, S. Pugazhendhi ,P. Sathyaand,  
R. Gopalakrishnan\*

Crystal Research Lab, Department of Physics, Anna University,  
Chennai – 600 025, India

\*Corres.author : krgkrishnan@annauniv.edu, krgkrishnan@yahoo.com  
Tel: +91-44-2235 8710 / 8707; Fax: +91-44-22358700

**Abstract :** A large size (25 mm length and 10 mm diameter) unidirectional LS single crystal has grown by unidirectional growth method of Sankaranarayanan-Ramasamy (SR) with a growth rate of 1.0 mm / day. The presence of functional groups in the grown crystal was identified from FT-IR and FT Raman spectrum studies. The transparency of the grown crystal was investigated by recording UV- Vis absorption spectrum and optical bandgap of the material was calculated. The dielectric permittivity, dielectric loss and conductivity over a range of frequencies and temperatures have been studied. The Vickers microhardness measurements were carried out on the <110>LS single crystal to estimate the mechanical properties. The growth mechanism was identified from the chemical etching studies.Z -scan reveals the third order nonlinearity of LS crystal.

**Keywords:** A1. Unidirectional crystal growth method; A1. Characterization; A1. Optical properties; B2. Dielectric properties; B2. Third order nonlinearity

### 1. Introduction

In recent years, various growth methods and apparatus have been continuously developed to improve the crystal quality and growth rate. Compared to other crystal growth techniques, the slow evaporation technique has been widely used to grow several types of crystals at ambient temperature. Orientation control during bulk crystal growth is one of the important development targets for crystal growers. Effective control of growth direction has attracted a great deal of attention. Therefore, technology for preparing bulk materials with effective orientation control has been required for achieving significant applications in the field of optoelectronics. In crystal growth literature, uniaxial solution-crystallization method of Sankaranarayanan - Ramasamy (SR) is a suitable method to effectively control the orientation of molecules during bulk crystal growth from solution at room temperature with 100% solute crystal conversion efficiency [1,2].

This method can be used to grow single crystal along the selected crystal direction, which is very important for the preparation of functional crystals. For example, as the conversion efficiency of SHG is always highest along the phase-match direction for nonlinear optical crystals. The unidirectional crystal growth method is the most suitable method for crystal growth along that direction.From this point of view, it is attempted to grow unidirectional, bulk, good quality single crystal of LS from its aqueous solution by unidirectional method. The grown crystals were subjected to various studies.

## 2. Experiments and Growth

### 2.1. Conventional Solution growth Method

Lithium Sulphanilate Hydrate (LS) was synthesized from the mixture of commercially available Sulphanilic acid and Lithium carbonate in a stoichiometric ratio of 1:1 at room temperature (35°C). The saturated solution of LS was prepared by dissolving the synthesized salt with continuous stirring of the solution using a magnetic stirrer at room temperature (35°C). On reaching saturation, the beaker containing the growth solution was optimally covered and housed in constant temperature bath( $\pm 0.01^\circ\text{C}$ ).

Lithium Sulphanilate Hydrate is an organic non-hygroscopic material. It has been grown by conventional slow evaporation solution technique (SEST), which belongs to monoclinic crystal structure with space group  $P2_1/c$  and the lattice parameters are  $a = 5.3430 (10) \text{ \AA}$ ,  $b = 7.9700 (10) \text{ \AA}$ ,  $c = 19.490 (3) \text{ \AA}$ ,  $\alpha = \gamma = 90^\circ$ ,  $\beta = 94.099 (10)^\circ$  and  $V = 827.8(2) \text{ \AA}^3$ . There are few reports available on the growth of LS in conventional method including its characterization [3,4]. Good transparent bulk single crystal of LS was harvested from mother solution after 40 days with a size of  $50 \times 10 \times 5 \text{ mm}^3$  and the crystal is shown in Figure 1.

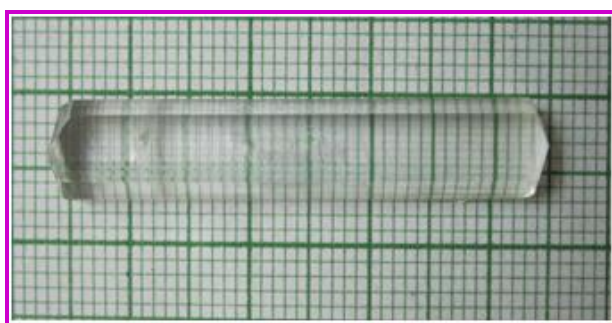


Figure 1 Conventional solution grown LS single crystal

### 2.2. Unidirectional Growth Method (SR Method)

The unidirectional LS single crystals were grown along the  $\langle 110 \rangle$  direction by mounting the dislocation-free seed crystal having (110) plane facing towards the saturated solution of LS in the growth ampoule. Then, the ampoule was filled with saturated solution of LS having optimized solute concentration and porously sealed; the schematic of experimental setup is as shown in Figure 2. A growth rate of 1.0 mm /day along the growth direction was observed. Growth rate of a uniaxial crystal of particular size along with a particular growth axis largely depends on the packing density of that plane, purity of the raw materials, degree of supersaturation and the rate of diffusion of the solute in the solvent medium. The harvested unidirectional grown crystal of LS is shown in Figure 3.

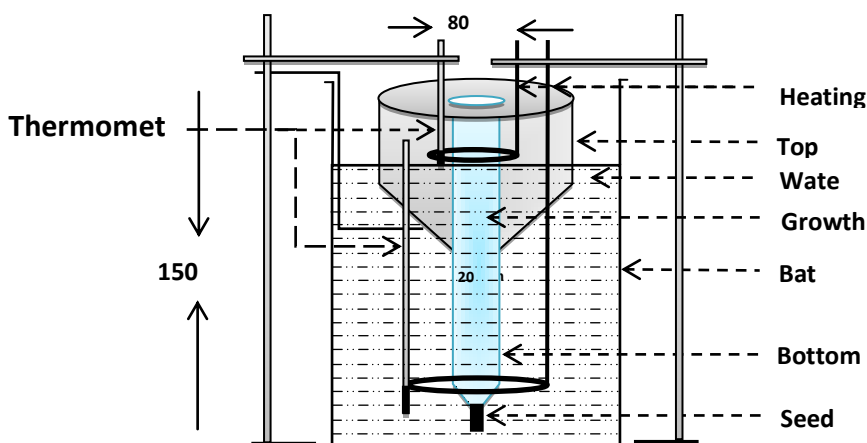


Figure 2 Schematic of Unidirectional growth setup



**Figure 3** <110> LS single crystal grown by Unidirectional method

In unidirectional method, since the crystal is growing in selective growth orientation, the commonly observed growth features in the case of conventional solution grown crystal such as growth sectors, growth boundaries, twins, stacking fault and dislocations are not observed in the X-ray topography [5]. This indicates that the unidirectional grown sample is relatively free from these defects.

### 3. Crystal Characterization

#### 3.1. Powder X-ray Diffraction Analysis

The grown Lithium Sulphanilate single crystal was subjected to Powder X-ray diffraction analysis using ENRAF NONIUS CAD4-F powder X-ray diffractometer with  $\text{CuK}\alpha$  ( $\lambda = 1.5418 \text{ \AA}$ ) radiation by crushing the LS crystal into fine powder. The sample was scanned over the range  $10 - 60^\circ$  at a rate of  $1^\circ / \text{min}$  which reveals well defined Bragg's peaks at specific  $2\theta$  angle and the crystallographic planes were indexed. The high intensity peak (110) plane is shown clearly in the powder XRD pattern (Figure 4).

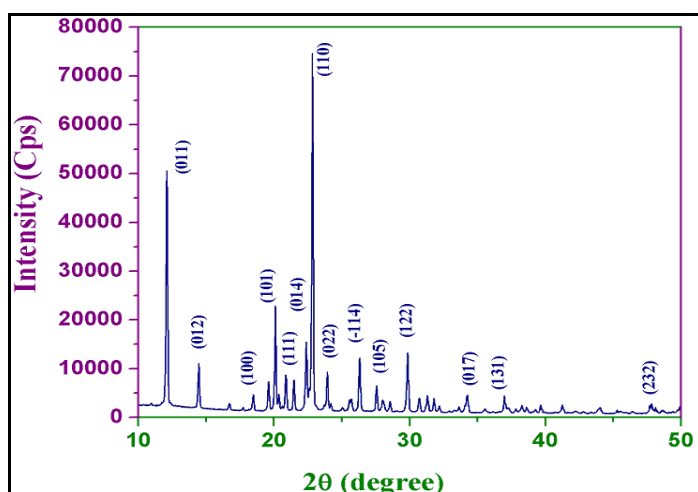


**Figure 4** Powder XRD pattern of LS crystal

#### 3.2. FTIR Analysis

The grown crystals were subjected to FTIR studies to analyze the functional groups quantitatively. The spectrum was recorded in the range  $500-4000 \text{ cm}^{-1}$  employing Bruker spectrometer by KBr Pellet method, resulting spectrum is as shown in Figure 5. The peaks observed at  $696 \text{ cm}^{-1}$  belongs to  $-\text{C}\equiv\text{C}-\text{H}$  alkynes groups whereas the peak observed at  $786, 836 \text{ cm}^{-1}$  correspond to aromatic group. Frequencies observed at  $1048 \text{ cm}^{-1}$  attributed as  $\text{C}-\text{N}$  stretching and  $1179 \text{ cm}^{-1}$  correspond to  $\text{C}-\text{H}$  wag ( $-\text{CH}_2\text{X}$ ) vibrations for alkyl halide group and  $1238 \text{ cm}^{-1}$  correspond to  $\text{S}=\text{O}$  stretching vibration is due to Sulfonate group.

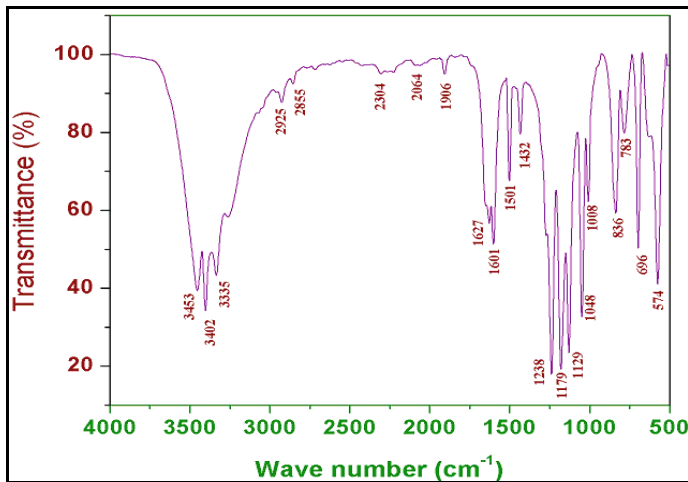


**Figure 5 FTIR spectrum of SR method grown LS**

The absorption peaks observed at 1432, 1501  $\text{cm}^{-1}$  correspond to N–O asymmetric stretch modes respectively for the nitro compound. The other peaks around 1601 and 1627  $\text{cm}^{-1}$  have been attributed to N–H bending vibration for amino compounds. The band appears at 2925  $\text{cm}^{-1}$  is attributed to H–C=O stretching vibration for aldehydes. In the present investigation, the O–H stretchings were observed at 3335, 3402 and 3453  $\text{cm}^{-1}$  which confirm the Alcohol groups present in the component. It shows that, the LS crystalline state exists as a dipolar ion in which the carboxylic group is present as a carboxylate ion and amino group is present.

### 3.3. UV–vis-NIR spectral analysis

The optical behaviour of the material basically includes the interaction of light radiation over the range of the electromagnetic spectrum. The ultraviolet light absorbed by the sample gives information about the transparency window which is very essential in many optoelectronic applications. The optical transmission and absorption spectra of Unidirectional grown crystals of good quality were recorded and the UV-vis-NIR spectra are as shown in Figure 6.

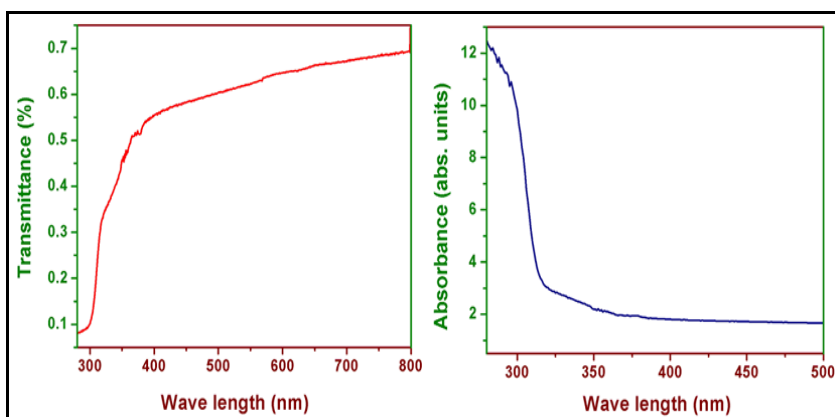


**Figure 6 UV-vis Transmission and absorption spectra of LS (110) single crystal**

As there is no absorption, the crystals were found to be transparent in the visible and near IR region, which is an essential parameter required for frequency doubling process [6]. With the wide transparency window in the entire visible and near IR range, these crystals can be used for optical device fabrication. The UV cut off wavelength of the LS single crystal is 320 nm and the percentage of transmittance of crystal is (~ 69%).

### 3.4. Bandgap measurement

The optical absorption coefficient ( $\alpha$ ) was calculated from the transmittance using the following relation,

$$\alpha = \frac{2.3036 \log\left(\frac{1}{T}\right)}{d} \quad (1.1)$$

where T is the transmittance and d is the thickness of the crystal. In the high photon energy region, the energy dependence of absorption coefficient suggests the occurrence of direct band gap. As a direct band gap the crystal under study has an absorption coefficient ( $\alpha$ ) obeying the following relation for high photon energies ( $h\nu$ ):

$$\alpha = \frac{A(h\nu - E_g)^{\frac{1}{2}}}{h\nu} \quad (1.2)$$

where  $E_g$  is the optical band gap of the crystal, and A is a constant. The variation of  $(h\nu)$  vs  $(\alpha h\nu)^2$  is shown in Figure 7.

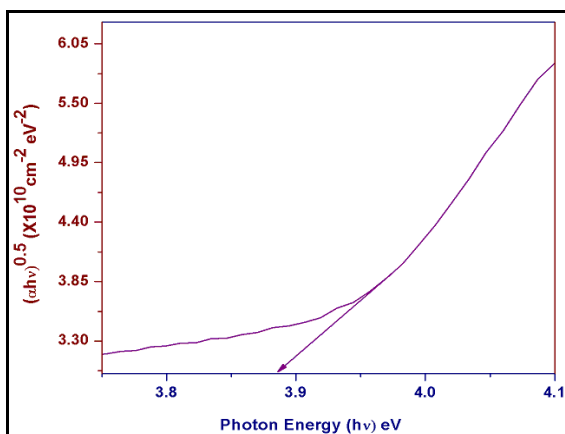


Figure 7 Band gap of LS (110) single crystal

The optical band gap is found to be 3.88 eV. As a consequence of wide band gap, the grown crystal has large transmittance in the visible region which enables these materials for higher harmonic generation [7].

### 3.5. Laser Raman Spectral Analysis

The Raman spectrum of LS was recorded between 200 and 1800  $\text{cm}^{-1}$ . The NH proton of LS molecule is sufficiently mobile to form strong hydrogen bonding interaction with the neighboring LS molecule in the crystal. This interaction may facilitate the centrosymmetric arrangement of LS in crystal lattice. The aromatic ring vibration produced a characteristic peak between 400 and 1600  $\text{cm}^{-1}$ . The laser Raman spectrum of LS is shown in Figure 8.

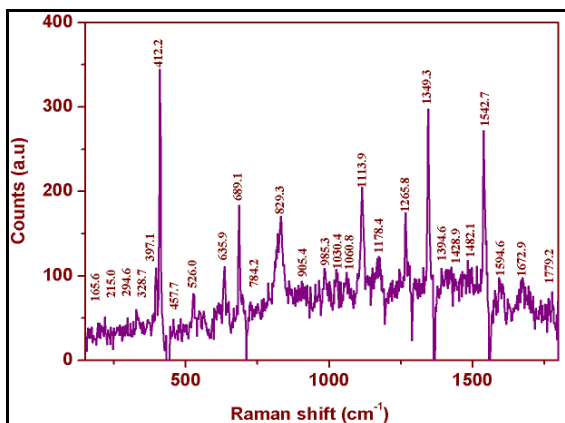


Figure 8 Laser Raman spectrum of LS

### 3.6. Photoluminescence (PL) Studies

The PL measurements were carried out using Jobin Yvon-spex spectrofluorometer (Fluorolog version – 3; Model FL3-11) with a xenon arc lamp (450 W) as excitation source which enclosed a PM tube (R 928) at the

detector side having a flat response 900 nm. In the present study the slit width is 2 nm. Photoluminescence (PL) is the spontaneous emission of light from a material under optical excitation. The photoluminescence spectrum was recorded for as-grown single crystal of LS at room temperature with an excitation wavelength of 316 nm as shown in Figure 9. A very strong and broad intense emission peak was observed at 559 nm which corresponds to near band-edge excitons of as-grown crystals. Moreover, absence of visible emission band indicates the high crystal quality and perfect crystallinity of as-grown crystals.

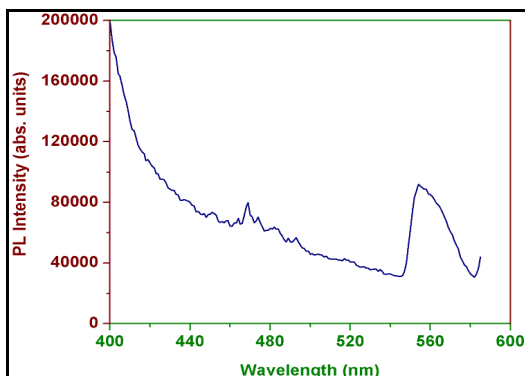


Figure 9 PL Spectrum for <110>LS single crystal

### 3.7. Microhardness Study

Microhardness indentations have been extensively applied at the microstructural level [8]. The mechanical stability is extremely important as far as the fabrication of devices is concerned. Hardness of a material is a measure of the resistance it offers to local deformation. LS single crystals with (110) plane was tested for their microhardness properties using a Vicker's indentation tester. The measurements were made at room temperature and the indentation time was kept at 5 sec. Vickers hardness (VHN) is given by the relation (1.3).

$$H_v = \frac{1.8544P}{d^2} \quad \left( \frac{g}{mm^2} \right) \quad (1.3)$$

where P is the test load in kg, d is the mean diagonal length of indentation in mm. Generally the hardness of the material varies with the applied load. The microhardness value was taken as the average of the several impressions made. The variation of hardness with indenter load for the grown single crystal is shown in Figure 10, which gives that the hardness value increases on increasing the load. The crystalline perfection was confirmed by the higher hardness value for the SR method grown LS crystal. The high mechanical hardness contributes to attractiveness of the present compound in practical applications.

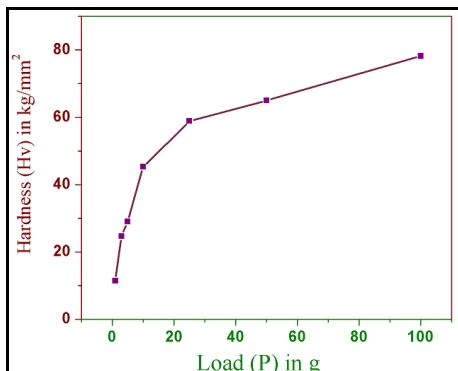


Figure 10 Microhardness of <110> LS single crystal

### 3.8. Dielectric Studies

The dielectric behaviour of the sample was studied at room temperature. The sample was electroded on either side with air-drying silver paste, so that it behaved like a parallel plate capacitor. The studies were carried out for the frequencies varying from 50 Hz to 5 MHz. The sample was mounted in a specially designed two

terminal sample holder made of stainless steel. The most important result concerns the determination of the role of hydrogen bonds in the appearance of the spontaneous polarization [9]. The frequency dependence of the dielectric permittivity is shown in Figure 11.

The capacitance of the crystal was measured to find out the relative dielectric permittivity.

$$\epsilon_r = \left( \frac{Cd}{A\epsilon_0} \right)$$

where  $\epsilon_r$  is the dielectric permittivity, C is the capacitance value of the crystal, A is the area of the crystal under investigation, d is the thickness of the sample used and  $\epsilon_0$  is the permittivity of free space. Dielectric permittivity and dielectric loss become nearly frequency independent; both these parameters gradually decrease with increase in the applied frequency as shown in Figure 12.

Due to electronic exchange of the number of ions in the crystal there is a local displacement of electrons in the direction of the applied field, which in turn gives rise to polarization. The dielectric permittivity of materials is due to the contribution of electronic, ionic, dipolar and space charge polarizations which depend on the frequencies. At low frequencies, all these polarizations are active. The space charge polarization is generally active at lower frequencies [10].

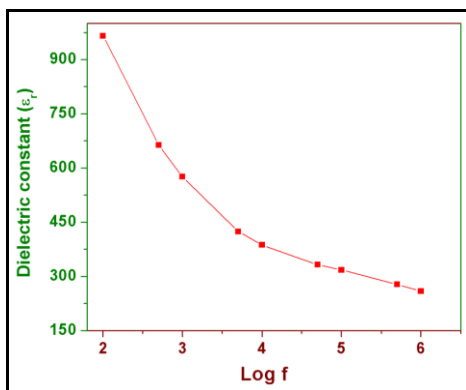


**Figure 11 Dielectric constant (vs log f) for <110>LS single crystal**

The characteristic of low dielectric constant and dielectric loss with high frequency for <110>LS single crystal suggests that the sample possesses enhanced optical quality with lesser defects and this parameter is of vital importance for various nonlinear optical materials and their applications.

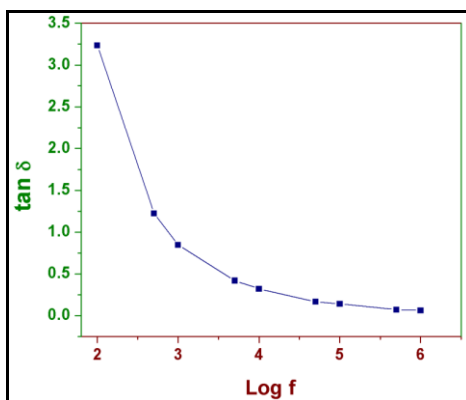


**Figure 12 Dielectric loss (vs log f) for (110) LS single crystal**

### 3.9. Etching Studies

The etching studies reveal the structural perfection and growth features of grown single crystal. The (110) face of conventional and SR grown LS crystals were subjected to etching with water at room temperature. The surface of conventional grown LS single crystal was completely immersed for 10 sec in the water etchant

for etching. The etched samples were dried using tissue paper and features were analyzed using a Magnus MLX microscope which represents the stacking type of etch pits and the number of etch pits is more as portrayed in the Figure 13.

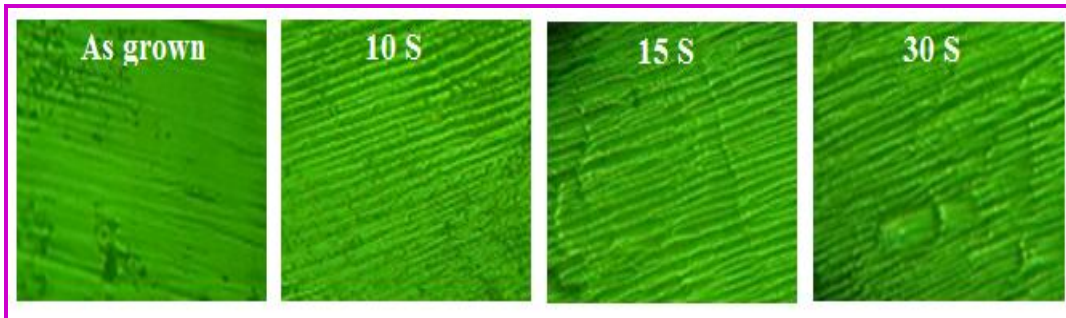


**Figure 13 Etched surfaces of (110) plane LS single crystal**

Further increasing the etching time to 10 sec, 15 sec and 30 sec, the pattern remains the same but the size of etch pits increases. When etching time increases the observed etch patterns are of well-defined shape. Less number of dislocations in (110) plane LS crystal shows that the quality of the crystals grown by SR method is better than conventional method grown LS crystal.

### 3.10 Z-SCAN STUDIES

The third order nonlinear refractive index and the nonlinear absorption coefficient were evaluated by Z-scan measurements. The typical Z-scan results of the LS single crystals are shown in Figure 14. The enhanced transmission near the focus suggests that there is a saturation of absorption at high intensity. Peak followed by valley in the closed aperture Z-scan plot indicates the defocusing effect, which may be due to thermal nonlinearity resulting from absorption of radiation at 532 nm. A spatial distribution of temperature was observed in all samples, which were produced due to the localized absorption of a tightly focused beam propagating through an absorbing sample medium. Hence, a spatial variation of the refractive index was produced which acted as a thermal lens resulting in phase distortion of the propagating beam. The difference in peak and valley transmission ( $\Delta T_{p-v}$ ) can be written in terms of the on-axis phase shift  $|\Delta \phi_0|$  at the focus as given in equation (1.4)

$$(\Delta T_{p-v}) = 0.406(1-S)^{0.25} |\Delta \phi_0| \tag{1.4}$$

where S is the Aperture Linear Transmittance and can be calculated using the relation  $S = 1 - \exp(-2r_a^2/w_a^2)$ . Here  $r_a$  is the aperture radius and  $w_a$  is the beam radius at the front of the detector. The nonlinear refractive index is given by the relation (1.5) [11].

$$n_2 = \frac{\Delta \phi_0}{k I_0 L_{eff}} \tag{1.5}$$

where,  $k = \frac{2\pi}{\lambda}$  ( $\lambda$  = laser wavelength)

$I_0$  Intensity of the laser beam at the focus ( $z = 0$ )

$$L_{eff} = \frac{1 - \exp(-\alpha L)}{\alpha}$$

is the effective thickness of the sample

$\alpha$  Linear absorption co-efficient

L is the thickness of the sample.

The nonlinear refractive index,  $n_2$  and the saturation absorption coefficient  $\beta$  can be determined by the measurements of the normalized transmittance versus sample position in closed and open aperture. Purely effective refractive index  $n_2$  is obtained by dividing closed aperture transmittance by corresponding open aperture transmittance. From the open aperture Z-scan data the nonlinear absorption co-efficient can be estimated using the relation (1.6).

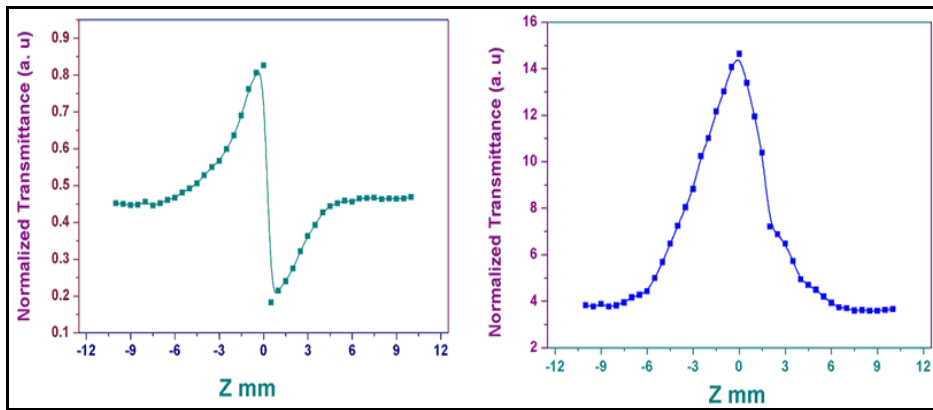


**Figure 14** Z-scan open and closed spectrum of LS single crystal

Figures 14 are the data of closed apertures Z-scan technique and open aperture Z-scan technique for the LS single crystals grown by conventional and unidirectional growth methods.

$$\beta = \frac{2\sqrt{2} \cdot \Delta T}{I_o L_{eff}} \tag{1.6}$$

The real and imaginary parts of the third-order nonlinear optical susceptibility  $\chi^{(3)}$  are defined as [12] given in equations (1.7) and (1.8)

$$\text{Re } \chi^{(3)} (\text{esu}) = 10^{-4} \frac{\epsilon_o C^2 n_o^2 n_2}{\pi} (\text{cm}^2 / \text{W}) \tag{1.7}$$

$$I_m \chi^{(3)} (\text{esu}) = 10^{-2} \frac{\epsilon_o C^2 n_o^2 \lambda \beta}{4\pi^2} (\text{cm} / \text{W}) \tag{1.8}$$

where  $\epsilon_0$  is the vacuum permittivity and  $c$  is the velocity of light in the vacuum.

**Table 1** Z scan data of LS <110> single crystal

Sample Name	Open aperture exp.		Closed aperture exp.			$\chi^{(3)} \times 10^{-6}$ (esu)
	$\Delta T$	$B \times 10^{-4}$ (cm/W)	$\Delta T_{p-v}$	$\Delta \phi_o$	$n_2 \times 10^{-9}$ (cm <sup>2</sup> /W)	
LS SR	0.4903	0.177	0.142	0.417	4.512	22.23

The results of Z-scan measurements of the samples are tabulated in Table 1. The peak–valley patterns of the normalized transmittance curve obtained under the closed aperture configuration reveal the characteristic self-defocusing behavior of the propagation in the samples, a property with wide application in the protection of optical sensors, like night-vision devices [12]. The high value of  $\chi^{(3)}$  is due to the  $\pi$ -electron cloud movement from donor to acceptor which can make the molecule highly polarized [13, 14].

#### 4. Conclusion

Good quality single crystal of LS was grown using a slow evaporation solution growth technique. Also a large size (25 mm length and 10 mm diameter), unidirectional single crystal of LS has been grown with a growth rate of 1.0 mm / day by Unidirectional growth method of Sankaranarayanan-Ramasamy (SR). Less etch pit density shows that the quality of the crystal grown by SR method is better than the conventional method grown crystal. The transmission spectrum reveals that the crystals have sufficient transmission in the entire visible region. The transmittance of conventional and unidirectional grown LS are 62% and 69%, respectively, and the UV cut-off wavelength is found to be 310 nm.

The frequency and temperature dependent dielectric constant and dielectric loss were studied. The self-defocusing and the nonlinear refraction as a function of intensity were observed for <110>LS single crystal in a Z-scan experiment with 532 nm He–Ne laser. The magnitudes for the real and imaginary parts of the third-order nonlinear susceptibility  $\chi^{(3)}$  ( $22.23 \times 10^{-6}$  esu) were calculated. The  $n_2$  and  $\beta$  values were found to be

$4.512 \times 10^{-9} \text{ cm}^2/\text{W}$  and  $0.177 \times 10^{-4} \text{ cm/W}$ , respectively. Z scan reveals that unidirectional grown LS crystal is suitable for NLO applications.

## References

1. Sankaranarayanan, K and Ramasamy, P 2005, 'Unidirectional seeded single crystal growth from solution of benzophenone', Journal of Crystal Growth, vol. 280, pp. 467-473.
2. Balamurugan, N and Ramasamy, P 2006, 'Investigation of the Growth Rate Formula and Bulk Laser Damage Threshold KDP Crystal Growth from Aqueous Solution by the Sankaranarayanan-Ramasamy (SR) Method', Crystal Growth and Design, vol. 6, pp. 1642-1644.
3. Anantharaja, M, and Gopalakrishnan, R, (2014), 'Studies on Lithium Sulphanilate Hydrate (LS) single crystal and its Characterization', International Journal of ChemTech Research, vol.6, no.1, pp. 222 – 235.
4. Haussühl, S 1997, 'Elastic properties of sulfanilates of Li, Na, K, Rb, Cs, Tl, NH<sub>4</sub>, CH<sub>3</sub>NH<sub>3</sub> and C(NH<sub>2</sub>)<sub>3</sub>', Zeitschrift für Kristallographie, vol. 212, issue 3, pp.186-190.
5. Anantharaja, M, Parthasarathy, M and Gopalakrishnan, R, (2013), 'Comparative studies on Growth and Characterization of sodium sulphanilate dihydrate single crystals from conventional solution growth and unidirectional growth method of Sankaranarayanan-Ramasamy', International Journal of ChemTech Research, vol.5, no.5, pp. 2636-2644.
6. Rao, CNR 1984, 'Ultraviolet and Visible Spectroscopy of Organic Compounds'. Prentice Hall Pvt. Ltd., New Delhi, pp. 60-66.
7. Krishnakumar, V, Manohar, S and Nagalakshmi, R 2010, 'Semioorganic nonlinear optical L-lysine sulphate growth and characterization', Spectrochim Acta A, vol. 75, pp. 1394-1397.
8. Leposava Sidjanina, Dragan Rajnovica, Jonjau Ranogajecb, 2007, Elvira Molnarb, 'Measurement of Vickers hardness on ceramic floor tiles' Journal of the European Ceramic Society, vol. 27, pp. 1767–1773.
9. Prasad, NV, Prasad, G, Bhimasankaran, T, Suryanarayana, SV and Kumar, G S 1996, 'Dielectric properties of cobalt doped cadmium oxalate crystals', Bulletin of Materials Science, vol. 19, pp. 639-643.
10. Smyth, CP 1965, 'Dielectric Behaviour and Structure', McGraw-Hill, New York.
11. Sheik Bahae, M, Said, AA and Van Stryland, EW 1989, 'High Sensitivity, Single Beam n<sub>2</sub> Measurements', Optics Letters, vol. 14, pp. 955-957.
12. Cassano, T, Tommasi, R, Ferrara, M, Babudri, F, Farinola, G M and Naso F 2001, 'Substituent-dependence of the optical nonlinearities in poly (2,5-dialkoxy-p-phenylenevinylene) polymers investigated by the Z-scan technique', Chem. Phys. Vol. 272, pp.111–118.
13. Yun-shan Zhou, En-bo Wang, Jun Peng, Jie Liu, Chang-wen Hu, Ru-danuang, and Xiaozeng You, 'Synthesis and the third-order optical nonlinearities of two novel charge-transfer complexes of a heteropoly blue type (C<sub>9</sub>H<sub>7</sub>NO)<sub>4</sub>H<sub>7</sub>PMO<sub>12</sub>O<sub>40</sub>·3H<sub>2</sub>O(C<sub>9</sub>H<sub>7</sub>NO=quinolin-8-ol) and (phen)<sub>3</sub> H<sub>7</sub>PMO<sub>12</sub>O<sub>40</sub>·CH<sub>3</sub>CN·H<sub>2</sub>O (phen=1,10-phenanthroline)', Polyhedron, vol.18, issue 10, pp. 1419–1423.
14. Chunying He, Yiqun Wu, Guang Shi, Wubiao Duan, Weina Song, Yinglin Song 2007, 'Large third-order optical nonlinearities of ultrathin films containing octacarboxylic copper phthalocyanine', Organic Electronics, vol. 8, Issues 2–3, pp. 198–205.

\*\*\*\*\*